

Shape reconstruction in 3D electromagnetic induction tomography using a level set technique

O. Dorn¹ and U. Ascher²

¹ Modeling and Numerical Simulation Group, Universidad Carlos III de Madrid, Leganes, Spain,
odorn@math.uc3m.es

³ Dept. Computer Science, University of British Columbia, Vancouver, Canada

Abstract

We present a novel shape reconstruction technique for 3D low frequency electromagnetic induction tomography which uses a level set representation of the shapes. An efficient adjoint scheme for calculating gradient directions corresponding to the data of each individual probing source is combined with a single-step technique for finding iterative corrections of the latest best guess of the level set function which defines the shapes. We present numerical experiments in 3D which demonstrate that our new technique is able to reconstruct complicated objects buried in the Earth from noisy electromagnetic data in a realistic geophysical setup without a priori knowledge of the topology of the shapes.

1 Introduction

Inverse problems for Maxwell's equations in 3D play an important role in a variety of important real-world applications, for example in non-destructive testing, for mine detection, in medical imaging, in the characterization of petroleum reservoirs or in the monitoring of pollutant plumes in the Earth. The majority of inversion codes nowadays still use lower-dimensional simplifications of the full 3D system of Maxwell's equations in order to invert the data. Even though these simplified models work well in some situations of special geometry, in the general case the results they yield are not satisfactory since the problem at hand is intrinsically 3D. We will present a new technique for the identification and characterization of geophysical shapes from low-frequency electromagnetic data which uses the full system of Maxwell's equations and a 3D level set technique for solving the inverse problem. The computational cost is reduced by employing a so-called *adjoint scheme* for calculating repeated corrections for an initial guess in an iterative manner. We show that our technique is able to reconstruct and characterize hidden shapes in 3D (as for example pollutant plumes in the Earth) from relatively few noisy electromagnetic data in a stable and efficient way for realistic geophysical situations.

2 The shape reconstruction problem

2.1 The forward problem

Assuming a time-dependence $e^{-i\omega t}$ for a given frequency $\omega = 2\pi f$, we consider the system of Maxwell's equations

$$\nabla \times \mathbf{E}_j(\mathbf{x}) - a(\mathbf{x})\mathbf{H}_j(\mathbf{x}) = \mathbf{M}_j(\mathbf{x}) \quad (1)$$

$$\nabla \times \mathbf{H}_j(\mathbf{x}) - b(\mathbf{x})\mathbf{E}_j(\mathbf{x}) = \mathbf{J}_j(\mathbf{x}) \quad (2)$$

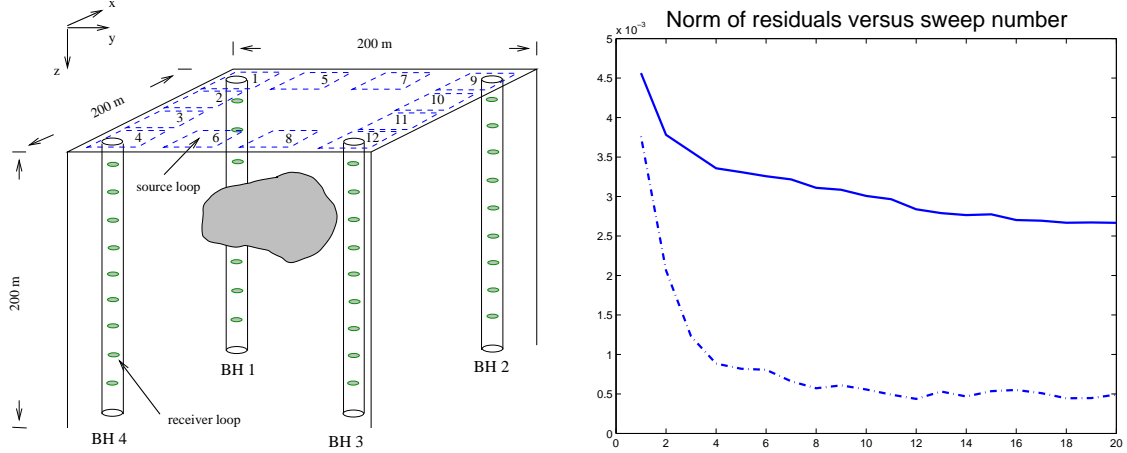


Figure 1: Left: computational setup. Right: evolution of cost. Solid line: data with 5% noise, with $\beta = 0.08$. Dash-dotted line: data without noise, using $\beta = 0$.

in a domain $\Omega \subset \mathbb{R}^3$, where $a(\mathbf{x}) = i\omega\mu(\mathbf{x})$ and $b(\mathbf{x}) = \sigma(\mathbf{x}) - i\omega\epsilon(\mathbf{x})$. We will assume that the parameters $a(\mathbf{x})$ and $b(\mathbf{x})$ are constant outside some sufficiently large ball with values denoted by a_0 and b_0 , respectively, and $\text{Re}(b_0) > 0$. With this assumption, we can apply some standard conditions on the propagation of the fields outside this ball. The index j in (1), (2) indicates the different applied source patterns for creating the electromagnetic fields. In this paper we consider the situation that the coefficient functions $a(\mathbf{x})$ and $b(\mathbf{x})$ contain discontinuities along closed interfaces $\Gamma \subset \Omega$.

In the inverse problem we are interested in estimating the unknown conductivity b from surface-to-borehole data. The permittivity ϵ and permeability μ are assumed to be known, which is a good approximation in various geophysical situations of low-frequency monitoring of conductive materials. For describing the interfaces in the domain we introduce a sufficiently smooth level set function $\phi : \Omega \rightarrow \mathbb{R}$ which defines the shape D by

$$b(\mathbf{x}) = \Pi(\phi)(\mathbf{x}) = \begin{cases} b_i(\mathbf{x}) & \text{in } D \text{ where } \phi(\mathbf{x}) \leq 0, \\ b_e(\mathbf{x}) & \text{in } \Omega \setminus D \text{ where } \phi(\mathbf{x}) > 0. \end{cases} \quad (3)$$

The boundary of the shape ∂D is given by the zero level set $\partial D = \{x \in \Omega : \phi(x) = 0\}$. We assume that we have p different sources \mathbf{q}_j , $j = 1, \dots, p$, which give rise to the fields \mathbf{E}_j and \mathbf{H}_j . The calculated data are $g_j(b) = \mathcal{M}_j \mathbf{E}_j$ where $\mathbf{E}_j, \mathbf{H}_j$ solve (1), (2) with parameter b and where \mathcal{M}_j is a (linear) measurement operator which depends on the source position. In our case, $\mathcal{M}_j \mathbf{E}_j$ are the line integrals of the electric fields along receiving closed wire loops inside the boreholes. We denote the actually measured (or 'true') data by \tilde{g}_j . Then, the residual operators $\mathcal{R}_j(b)$ and $\mathcal{T}_j(\phi)$ are defined as

$$\mathcal{R}_j(b) = g_j(b) - \tilde{g}_j, \quad \mathcal{T}_j(\phi) = \mathcal{R}_j(\Pi(\phi)) \quad (4)$$

2.2 Gradient calculations by an adjoint scheme

Defining the least squares cost functionals $\mathcal{J}_j(b) = \frac{1}{2} \|\mathcal{R}_j(b)\|_2^2$, and $\hat{\mathcal{J}}_j(\phi) = \frac{1}{2} \|\mathcal{T}_j(\phi)\|_2^2$, we call

$$\text{grad}_{\mathcal{J}_j, L_2}(b) = \mathcal{R}'_j(b)^* \mathcal{R}_j(b), \quad \text{grad}_{\hat{\mathcal{J}}_j, L_2}(\phi) = \mathcal{T}'_j(\phi)^* \mathcal{T}_j(\phi) \quad (5)$$

the *gradient directions* of \mathcal{J}_j in b and ϕ , respectively. Notice that these gradient directions will depend on the choice of function spaces for the parameter functions b and level set functions ϕ , as indicated in the notation. This will be used when selecting our regularization scheme for the inversion. We have the following *adjoint representation of $\mathbf{grad}_{\mathcal{J}_j, L_2}(b)$* as shown for example in [1].

Let \mathbf{E}_j^a and \mathbf{H}_j^a be the solution of the following (adjoint) system of Maxwell's equations:

$$\nabla \times \mathbf{E}_j^a(\mathbf{x}) - a(\mathbf{x})\mathbf{H}_j^a(\mathbf{x}) = 0 \quad (6)$$

$$\nabla \times \mathbf{H}_j^a(\mathbf{x}) - b(\mathbf{x})\overline{\mathbf{E}_j^a(\mathbf{x})} = \mathcal{M}_j^* \overline{\mathcal{R}_j(b)} \quad (7)$$

where \mathcal{M}_j^* denotes the formal adjoint of the measurement operator \mathcal{M}_j . Its application amounts to putting the argument (here $\overline{\mathcal{R}_j(b)}$) as artificial 'adjoint sources' at the receiver locations. The overline denotes 'complex conjugate'. Then we have

$$\left[\mathcal{R}'_j(b)^* \mathcal{R}_j(b) \right] (\mathbf{x}) = \overline{\mathbf{E}_j(\mathbf{x}) \cdot \mathbf{E}_j^a(\mathbf{x})} \quad (8)$$

where \mathbf{E}_j and \mathbf{H}_j are the solution of (1), (2) with b .

Formal differentiation by the chain rule yields $\mathcal{T}'_j(\phi) = \mathcal{R}'_j(\Pi_j(\phi))\Pi'_j(\phi)$. We have $\Pi'_j(\phi) = (b_i - b_e)\delta(\phi)$. However, the Dirac delta distribution $\delta(\phi)$ will be considered to be approximated by a suitable L_2 -function. In our numerical implementations, we will use the narrowband function of thickness d for that purpose. In other words, $\delta(\phi) \approx \chi_{B_d(\Gamma)}$ with $B_d(\Gamma) = \{\mathbf{x} : \text{dist}(\mathbf{x}, \Gamma) \leq d/2\}$ and χ_D denoting the characteristic function of the set D . We have

$$\mathcal{T}'_j(\phi)^* = \Pi'_j(\phi)^* \mathcal{R}'_j(\Pi(\phi))^*.$$

Notice that so far no regularization scheme is applied in order to stabilize the inversion. A popular scheme would be to add an additional term to the cost functional $\mathcal{J}_j(b)$ which will give us additional terms to the gradient directions. However, here we have decided to try a different route. We implicitly regularize the inversion by enforcing that the individual updates of the level set function are 'projected' towards a smoother function space in the following manner. Assuming that $\phi \in W_1(\Omega)$ with

$$\begin{aligned} W_1(\Omega) &= \{ \phi : \phi \in L_2(\Omega), \nabla \phi \in L_2(\Omega), \frac{\partial \phi}{\partial \nu} = 0 \text{ at } \partial \Omega \} \\ \langle v, w \rangle_{W_1(\Omega)} &= \alpha \langle v, w \rangle_{L_2(\Omega)} + \beta \langle \nabla v, \nabla w \rangle_{L_2(\Omega)} \end{aligned}$$

we replace the adjoint operator $\mathcal{T}'(\phi)^*$ by a new adjoint operator $\mathcal{T}'_j(\phi)^\circ$ which maps back from the data space into this space $W_1(\Omega)$ with its associated weighted inner product $\langle v, w \rangle_{W_1(\Omega)}$ and $\alpha \geq 1$ and $\beta > 0$ being carefully chosen regularization parameters. Following these lines we arrive at the new gradient directions

$$\mathcal{T}'_j(\phi)^\circ = (\alpha I - \beta \Delta)^{-1} \mathcal{T}'_j(\phi)^*, \quad \mathbf{grad}_{\mathcal{J}_j, W_1}(\phi) = \mathcal{T}'_j(\phi)^\circ \mathcal{T}_j(\phi). \quad (9)$$

See, e.g., [2] for details. The positive definite operator $(\alpha I - \beta \Delta)^{-1}$ has the effect of 'projecting' the gradient $\mathcal{T}'_j(\phi)^* \mathcal{T}_j(\phi)$ from $L_2(\Omega)$ towards the smaller space $W_1(\Omega)$. In fact, different choices of the weighting parameters α and β visually have the effect of 'smearing out' the unregularized updates to a different degree. In particular, high frequency oscillations or discontinuities of the updates for the level set function are removed, which yields shapes with more regular boundaries. We will use this gradient direction in order to design our nonlinear single-step reconstruction scheme as follows. See also the general discussions on regularization schemes led in [2, 5].

2.3 The shape reconstruction algorithm

We have calculated in the previous subsection gradient directions with respect to the individual cost functionals $\mathcal{J}_j(b)$ which only take into account the part of the complete data set which corresponds to source \mathbf{q}_j . The gradient direction which corresponds to the full data set would be a vector whose components are the individual gradient directions $\mathbf{grad}_{\hat{\mathcal{J}}_j, W_1}(\phi)$. However, calculating this combined gradient vector in each step of an iterative reconstruction technique is quite expensive in this case of 3D Maxwell's equations. Therefore, we have adopted in our inversion a single-step reconstruction scheme which follows the general single-step idea of the nonlinear Algebraic Reconstruction Technique (ART) as described in [4]. We perform so-called 'sweeps' over the source positions and only consider the information of one source at a time while calculating an update by an efficient adjoint scheme. The algorithm reads as follows.

Algorithm: Single step level set shape reconstruction technique

Initialization:

Define initial level set function as a signed distance function $\phi^{(0)}$ and put $n = 0$.

Reconstruction:

FOR $m = 1 : M$ (loop over sweeps)

FOR $j = 1 : p$ (loop over source positions)

Calculate $\mathbf{grad}_{\hat{\mathcal{J}}_j, W_1}(\phi^{(n)}) = \mathcal{T}'_j(\phi^{(n)}) \circ \mathcal{T}_j(\phi^{(n)})$ by (6)-(9)

Update level set function: $\phi^{(n+1)} = \phi^{(n)} - \gamma \mathbf{grad}_{\hat{\mathcal{J}}_j, W_1}(\phi^{(n)})$
with step-size $\gamma > 0$

Rescale $\phi^{(n+1)} \rightarrow \zeta \phi^{(n+1)}$ with scaling parameter $\zeta \in \mathbf{R}^+$.

END

Verify optional stopping criterion.

END

3 Numerical experiments

In our numerical experiments we use 12 large wire loop sources which are located slightly above the air-soil interface and which are arranged as shown in the left image of Fig.1. Each of these wire loops has 45 m side-length. The search domain has the size $200 \times 200 \times 200 \text{ m}^3$. We use a relatively low frequency of 1 KHz in order to have electromagnetic fields which can penetrate large distances in the Earth. However, this also makes the inverse problem more ill-posed: the expected resolution is quite low due to the diffusive behavior of the fields and due to the relatively limited view. In each of the 4 boreholes shown in Fig.1, 20 receivers are deployed equidistantly. They measure line integrals of the electric fields along small wire loops. Then, 0.5 % of Gaussian noise is added to real and imaginary parts of each data value. The conductivity in the air is assumed to be $\sigma = 10^{-8}$ Siemens/m (S/m), in the soil $\sigma = 0.1$ S/m, and inside the unknown inhomogeneities embedded in the soil $\sigma = 0.5$ S/m. The permittivity and permeability are constant in the domain with values $\epsilon_r = 1$ and $\mu_0 = 4\pi \times 10^{-7} \text{ WbA}^{-1}\text{m}^{-1}$, respectively. All parameters are assumed to

be known in the reconstruction. Extensions of our technique to the simultaneous reconstruction of these values and the corresponding shape seem possible, see the discussion in [2], but will not be considered here. The true reference profile which needs to be reconstructed from the gathered data consists of two blocks (which could represent for example contaminant fluid plumes) embedded in the background soil and is shown in the bottom right image of Fig.2. The starting guess for our reconstruction is a small blob at some central location of the search domain as shown in the top left image of Fig.2, modeled by a corresponding signed-distance level set function. The algorithm uses a narrowband whose width d is 3 voxel-sizes. The parameters α and β have been chosen as $\alpha = 1$ and $\beta = 0.08$. The step-size γ is chosen empirically during the first sweep, and is then kept fixed throughout the reconstruction. The scaling factor ζ is chosen in each step of the algorithm individually such that the total minimum of the rescaled level set function has the value -10 . A finite-volume discretization is used for solving the forward and adjoint problems in each step of the algorithm. See [3] for details of this scheme.

The reconstructed shapes for several of the 20 sweeps of the algorithm are displayed in the top and bottom row of Fig.2. Fig.1 shows on the right the evolution of the cost during the reconstruction (solid line). We observe that the cost decreases in a continuous and stable way until reaching a low practically stationary level. Here the algorithm stopped in our implementation due to the stationary cost value. For comparison, we have displayed in Fig.3 the evolution for the same situation but now without noise in the data and without applying regularization (i.e., choosing $\beta = 0$). Even though no noise was added to the data, such that the final cost value is smaller than before (see the dash-dotted line in the plot of Fig.1), the reconstruction is not as good now due to the irregularity of the recovered shape.

Acknowledgment

The authors thank D. Oldenburg and E. Haber for useful discussions.

References

- [1] O. Dorn, H. Bertete-Aguirre, J.G. Berryman and G.C. Papanicolaou 1999 A nonlinear inversion method for 3D electromagnetic imaging using adjoint fields, *Inverse Problems* **15** 1523-1558.
- [2] O. Dorn and D. Lesselier 2006 Level set methods for inverse scattering *Topical Review, Inverse Problems* **22** R67–R131.
- [3] E. Haber and U. Ascher 2001 Fast finite volume simulation of 3D electromagnetic problems with highly discontinuous coefficients, *SIAM J. Sci. Comput.* **6** 1943-1961.
- [4] F. Natterer and F. Wübbeling 2001 *Mathematical Methods in Image Reconstruction* (SIAM: Philadelphia).
- [5] K. van den Doel and U. Ascher 2006 On level set regularization for highly ill-posed distributed parameter estimation problems *J. Comp. Phys.* **216** 707-723.

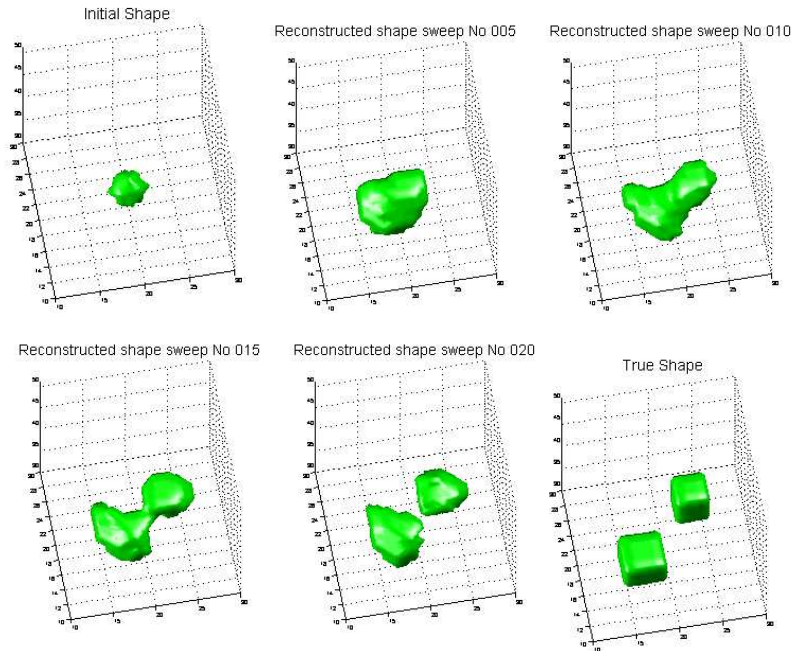


Figure 2: Data with 0.5 % noise, using $\alpha = 1$, $\beta = 0.08$. Top row from left to right: initial guess, reconstructions after 5 and 10 sweeps. Bottom row from left to right: Reconstruction after 15 and 20 sweeps; true reference model.

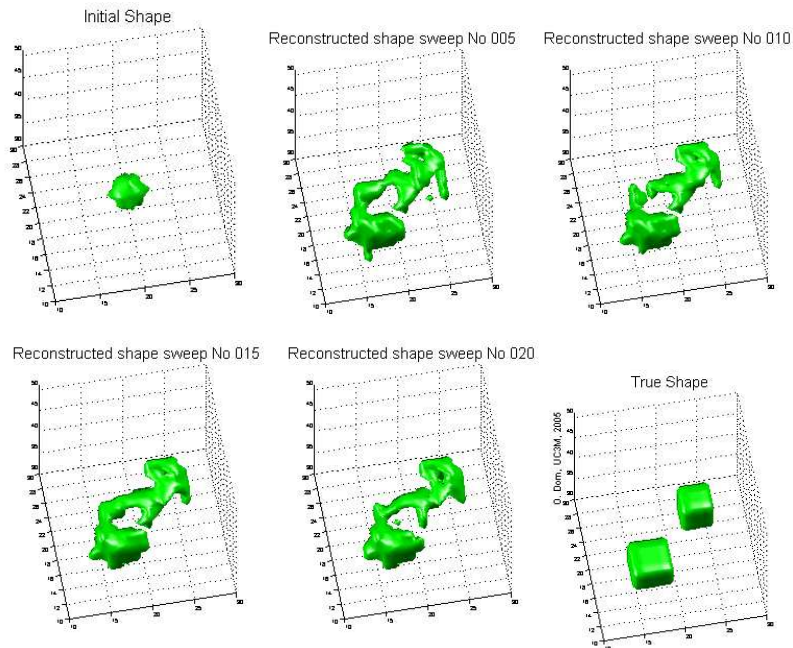


Figure 3: Data without noise, with $\alpha = 1$, $\beta = 0$. Top row from left to right: initial guess, reconstructions after 5 and 10 sweeps. Bottom row from left to right: Reconstruction after 15 and 20 sweeps; true reference model.